Pathway of Promoter Melting by *Bacillus subtilis* RNA Polymerase at a Stable RNA Promoter: Effects of Temperature, δ Protein, and σ Factor Mutations†

Yue-Li Juang and John D. Helmann*

Section of Microbiology, Cornell University, Ithaca, New York 14853-8101

Received February 22, 1995; Revised Manuscript Received April 21, 1995®

ABSTRACT: *Bacillus subtilis* RNA polymerase (RNAP) contains a catalytic core ($\beta\beta'\alpha_2$; or E) associated with one of several σ factors, which determine promoter recognition, and δ protein, which enhances promoter selectivity. We have shown previously that specific mutations in σ^A region 2.3, or addition of δ, decrease the ability of RNAP to melt the *ilv-leu* promoter. Here we extend these studies to a stable RNA promoter, P_{trnS}, which controls transcription of seven tRNA genes. $KMnO_4$ footprinting was used to visualize DNA melting at P_{trnS} as a function of both temperature and the protein composition of the RNAP holoenzyme. We propose that the pathway leading to productive initiation includes several intermediates: a closed complex (RP_c), a complex in which DNA melting has nucleated within the conserved TATA element (RP_n), and an open complex in which DNA-melting extends to at least −4 (RP_{o1}). RNAP reconstituted with either of two mutant σ^A proteins, Y189A and W192A, was defective for both the nucleation and propagation of the transcription bubble while a third σ^A mutant, W193A, allows normal nucleation of DNA-melting, but does not efficiently propagate the melted region downstream.

Transcription initiation is a multistep reaction which includes several common intermediates. The initial promoter-bound closed complex (RP_c) isomerizes in one or more steps to the strand-separated open complex (RP_o) (Buc & McClure, 1985; Leirmo & Record, 1990; Roe *et al.*, 1985). In the presence of ribonucleoside triphosphate (NTP)[1] substrates, RNA polymerase (RNAP) synthesizes and releases short RNA chains in an abortive synthesis reaction (Carpousis & Gralla, 1980; Munson & Reznikoff, 1981). These initial transcribing complexes (RP_{ITC}) still contain the σ subunit and are in equilibrium with RP_o (Krummel & Chamberlin, 1989). With a variable probability, the RNA chain achieves a length, typically around 10 nucleotides (Hansen & McClure, 1980; Stackhouse *et al.*, 1989), which triggers a large conformation change which converts the relatively unstable RP_{ITC} into a stable elongation complex (RP_e). This process is referred to as promoter clearance and can be rate-limiting both *in vitro* and *in vivo* (Ellinger *et al.*, 1994a,b; Knaus & Bujard, 1988, 1990).

The pathway of transcription initiation has been most intensively studied for the *Escherichia coli* RNAP (Leirmo & Record, 1990). At many strong *E. coli* promoters, RNAP forms stable open complexes, and the promoter melting step is essentially irreversible. However, at *E. coli rrn* promoters, RNAP does not form stable open complexes, and the polymerization of the first two initiating nucleotides is required for stabilization of the strand-separated intermediate (Gourse, 1988; Ohlsen & Gralla, 1992a,b). *Bacillus subtilis* RNAP also does not generally form stable binary complexes (Dobinson & Spiegelman, 1987; Juang & Helmann, 1994a; Whipple & Sonenshein, 1992). For example, open complexes at the very strong φ29 promoter, P_{A2b}, are heparin-sensitive on linear DNA unless the first phosphodiester bond is formed (Rojo *et al.*, 1993). Even when a strand-separated open complex can be demonstrated, *B. subtilis* RNAP is readily displaced by heparin or by competing DNA templates which suggests that there is a rapid equilibrium between open complexes, closed complexes, and free RNAP (Whipple & Sonenshein, 1992).

We previously characterized intermediates in transcription initiation by *B. subtilis* RNAP on the *ilv-leu* promoter (P_{ilv}) (Juang & Helmann, 1994b). At this promoter, $E\sigma^A$ forms open complexes while RNAP containing δ ($E\sigma^A\delta$) forms predominantly closed complexes even at 40 °C (Juang & Helmann, 1994a). Despite this inhibition of promoter melting, δ increased RNA synthesis by 4-fold in a multiple cycle reaction, suggesting that a slow step, postulated to be the recycling of core enzyme, was stimulated by δ. At P_{ilv}, we demonstrated that several σ^A region 2.3 mutants impaired transcription initiation at the promoter melting step; reconstituted mutant RNAP ($E\sigma^A$) formed predominantly closed complexes even at 40 °C, and although they retained transcriptional activity, their activity was cold-sensitive relative to that of wild-type $E\sigma^A$ RNAP (Juang & Helmann, 1994b). As expected for a melting defect, DNA supercoiling suppressed and δ exacerbated this low-temperature transcriptional defect.

We now extend our analysis of transcription initiation to the strong P_{trnS} promoter, containing consensus −35 and −10 elements and an optimal 17 bp spacer, which directs transcription of an operon of seven tRNA genes (Garrity & Zahler, 1993). Our analysis leads us to propose a pathway of transcription initiation involving an initial closed complex (RP_c), an intermediate complex in which DNA-melting has nucleated within the conserved TATA element (RP_n), and a partially opened complex (RP_{o1}) in which melting has propagated near, but apparently not past, the transcription

† This research was supported by Grant GM 47446 from the National Institutes of Health.

* Author to whom correspondence should be addressed. Telephone: 607-255-6570. FAX: 607-255-3904. Email: jdh9@cornell.edu.

® Abstract published in *Advance ACS Abstracts,* June 15, 1995.

[1] Abbreviations: bp, base pair(s); nt, nucleotide(s); NTP, ribonucleoside triphosphate.

0006-2960/95/0434-8465$09.00/0

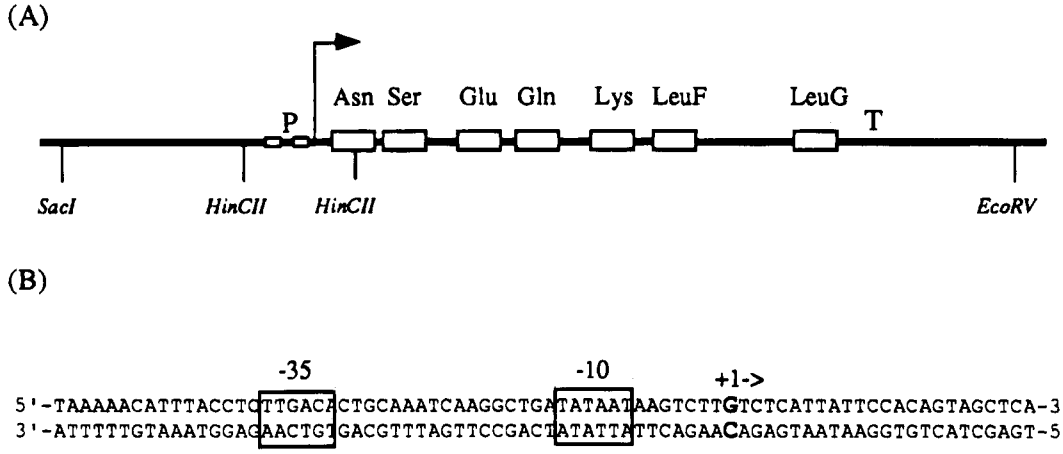

FIGURE 1: Diagrams of the *B. subtilis trnS* operon (Garrity & Zahler, 1994) and the promoter sequence of P_{trnS}. (A) The 1237 bp *Sac*I–*Eco*RV *trnS* operon DNA fragment used for *in vitro* transcription. P stands for promoter, T stands for terminator, and the arrow represents the direction of transcription. The large boxes represent the seven tRNA genes, and the small boxes represent the −35 and −10 regions of P_{trnS}. (B) The DNA sequence of P_{trnS} with the transcription start site (G) indicated in boldface.

start site. The presence of initiating substrates allows the visualization of DNA-melting around the transcription start point, suggesting that the nascent transcript may stabilize melting of the start site region.

EXPERIMENTAL PROCEDURES

Purification of Core RNA Polymerase, σ^A Proteins, and δ. The purification of wild-type and mutant σ proteins, core RNA polymerase containing δ (Eδ), and core RNA polymerase lacking δ (E) was performed as described (Juang & Helmann, 1994a). δ was obtained by purification from an *E. coli* strain engineered to overproduce δ (F. Lopez de Saro and J. D. Helmann, unpublished results).

In Vitro Transcription. A 1237 bp *Sac*I–*Eco*RV DNA fragment containing the *trnS* operon was isolated from pDG200 (Garrity & Zahler, 1993) and cloned into pBSK$^+$ to generate pTRNS. This DNA fragment was purified from pTRNS by 4% polyacrylamide gel electrophoresis and elution as described (Juang & Helmann, 1994a). Transcription assays (25 μl) were performed as described (Juang & Helmann, 1994b) using 0.3 pmol of DNA template and reconstituted RNAP (containing 1.5 pmol of core enzyme, 13 pmol of σ^A, and, where indicated, 13 pmol of δ). Transcription buffer contained 18 mM Tris-HCl (pH 8.0 at 25 °C), 10 mM $MgCl_2$, 10 mM NaCl, 20 μM EDTA, 10% (v/v) glycerol, 8 mM 2-mercaptoethanol and NTPs as indicated.

Footprinting Reactions. For DNase I and $KMnO_4$ footprinting, the 1237 bp P_{trnS} promoter fragment (see above) was digested with *Hin*cII, and the resulting 149 bp fragment, extending from −104 to +45 relative to the *trnS* transcription start site, was purified and cloned into the *Sma*I site of pBSK+. The resulting plasmid, pYLJ18, contains the P_{trnS} promoter region oriented toward the polylinker *Eco*RI site. For the nontemplate strand, a 5′ end-labeled P_{trnS} DNA fragment was prepared as described except that *Acc*I was replaced by *Bsp*120I (Juang & Helmann, 1994b). To label the template strand at the 3′ end, *Eag*I-digested pYLJ18 was treated with [α-^{32}P]dGTP and the Klenow fragment of DNA polymerase I for 15 min at room temperature, and then a mixture of all four dNTPs (unlabeled) was added for an additional 5 min. DNA fragments labeled on either the template or the nontemplate strand were purified by preparative polyacrylamide gel electrophoresis as described (Juang & Helmann, 1994a).

Footprinting experiments were performed in transcription buffer containing either 2 mM DTT (for $KMnO_4$ footprinting) or 8 mM 2-mercaptoethanol (for DNase I footprinting). When indicated, the Tris-HCl buffer was replaced with 20 mM Na·Hepes (pH 8.0 at 25 °C). Eσ^A and E$\delta\sigma^A$ were reconstituted as described in the *in vitro* transcription assays. To quantify the intensity of the permanganate signals under different conditions, radioactivity was measured using a Molecular Dynamics phosphorimaging system and ImageQuant data analysis software. Background reactivity, corresponding to the signal at the same temperature in the absence of added protein, was subtracted, and each signal was normalized against a control band (or bands) which did not exhibit RNAP-dependent changes in reactivity.

RESULTS

DNA-Melting at P_{trnS} by Eσ^A and E$\sigma^A\delta$ as a Function of Temperature. We used the single-strand-selective reagent potassium permanganate ($KMnO_4$) to modify exposed thymines within open complexes formed at P_{trnS} (Figure 1). At 40 °C, both the Eσ^A and E$\sigma^A\delta$ enzymes induced thymine reactivity at positions −11 and −4 on the nontemplate strand, and at positions −10 and −12 on the template strand (Figures 2 and 3). At lower temperatures, thymine reactivity was reduced, which indicates that the proportion of binary RNAP–promoter complexes in the open state was decreased. In the course of these studies, we unexpectedly observed that the pattern and extent of permanganate reactivity were reproducibly altered if Tris-HCl was replaced by Na·Hepes in the incubation buffer (compare Figures 2 and 3).

To quantify the extent of DNA-melting under these various conditions, we measured the intensity of the −12, −11, and −4 thymine signals using phosphorimage analysis. A plot of the relative permanganate reactivity vs temperature (Figure 4) indicated a transition temperature of 25 °C for melting of P_{trnS} by Eσ^A in Tris-HCl buffer (Figure 4A; see Experimental Procedures). The relative reactivity at each of these three thymines (−12, −11, and −4) increased in parallel, consistent with a cooperative melting over this region of the DNA. In the presence of δ, the thymine reactivity was reduced by nearly 3-fold even at 40 °C (Figure 4B), which suggests that

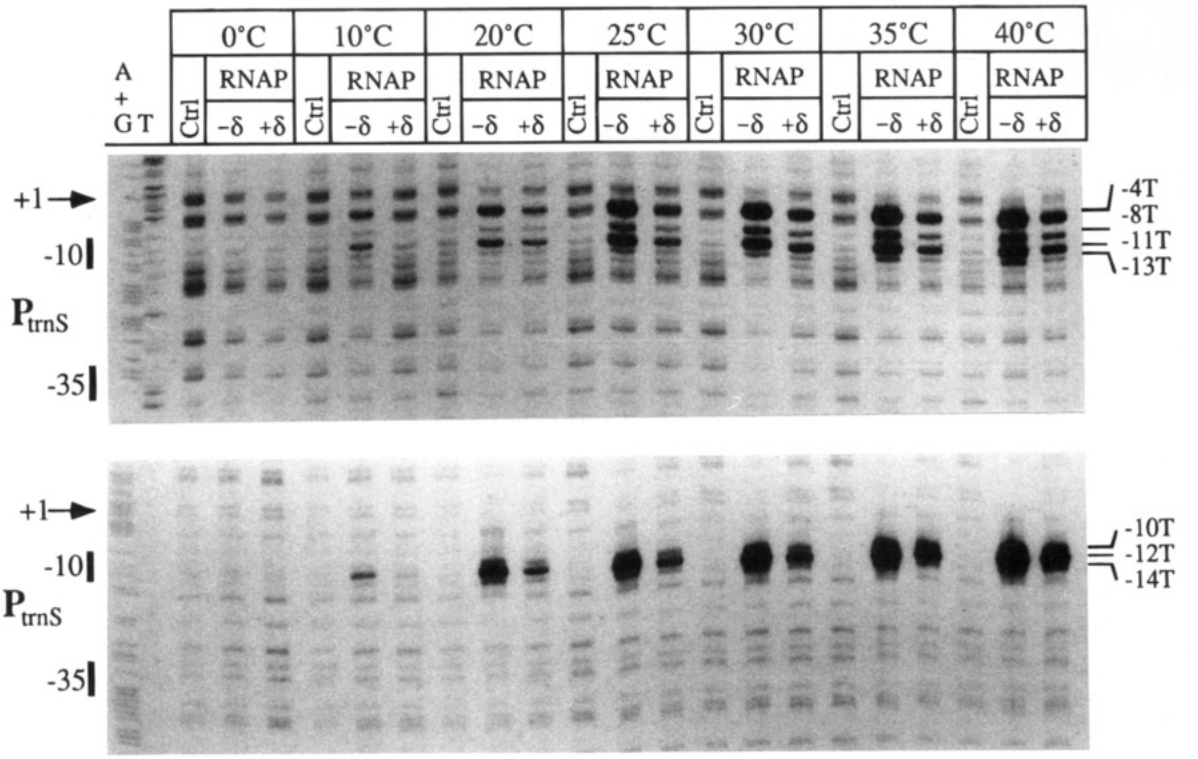

FIGURE 2: $KMnO_4$ footprinting of RNAP−promoter complexes in Tris-HCl buffer (pH 8.0 at 25 °C). RNAP was incubated at the indicated temperature with P_{trnS} DNA which was labeled on the 5′-end of the nontemplate strand (top panel) or the 3′-end of the template strand (bottom panel) prior to reaction with $KMnO_4$. The numbers indicate the positions of reactive thymines relative to the transcription start site of P_{trnS}. Maxam−Gilbert sequencing reactions for A+G or T were used as markers.

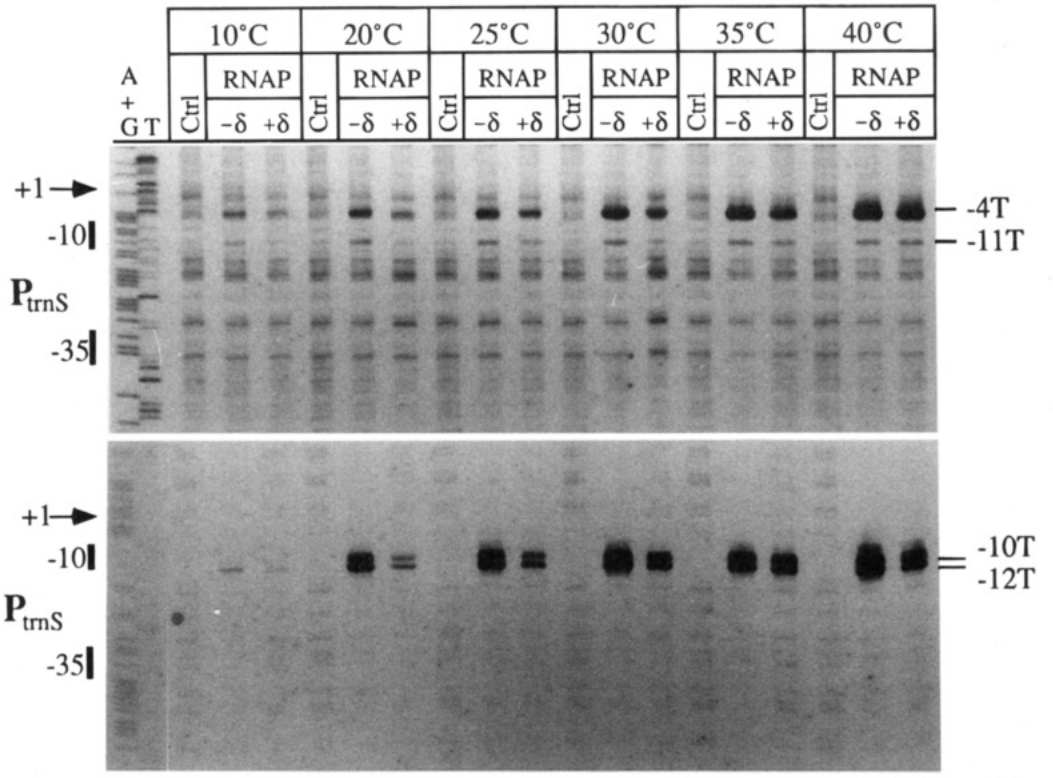

FIGURE 3: $KMnO_4$ footprinting of RNAP−promoter complexes in Na·Hepes buffer (pH 8.0 at 25 °C). RNAP−P_{trnS} DNA complexes were prepared and treated with $KMnO_4$ as described for Figure 2 except that Tris-HCl buffer was replaced by Na•Hepes. Top panel, nontemplate strand; bottom panel, template strand.

the transition temperature is >40 °C under these conditions. This is consistent with our previous observation that δ greatly increases the transition temperature for the *ilv-leu* promoter: E$\sigma^A\delta$ forms closed complexes even at 40 °C (Juang & Helmann, 1994a). In general, a comparison of the complexes formed at P_{trnS} and P_{ilv}, both in the presence and in the absence of δ, suggests that DNA-melting is more facile at P_{trns}.

When permanganate reactivity was measured in Na·Hepes buffer, a different picture emerged (Figure 3). First, overall

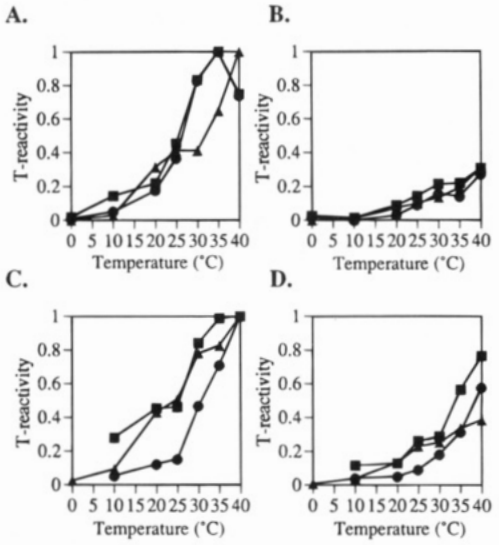

FIGURE 4: $KMnO_4$ reactivity vs temperature for binary RNAP−P_{trns} complexes. Reactivity of thymines at −11 (B) and −4 (J) on the nontemplate strand and −12 (H) on the template strand for (A) Eσ^A RNAP, Tris-HCl buffer; (B) E$\sigma^A\delta$ RNAP, Tris-HCl buffer; (C) Eσ^A RNAP, Na•Hepes buffer; or (D) E$\sigma^A\delta$ RNAP, Na•Hepes buffer. The data of Figures 3 and 4 were quantified by phosphorimager analysis, and the signal intensities were normalized against the maximal reactivity displayed by Eσ^A. In each case, background reactivity (as determined from the no protein control lanes) has been subtracted.

reactivity was reduced relative to Tris-HCl buffer. Second, several thymines which were permanganate-reactive in Tris-HCl were not reactive in the complexes formed in Na•Hepes (e.g., −8 on the nontemplate strand and −14 on the template strand). Third, and most striking, melting now occurred in a stepwise, rather than a concerted, fashion. For example, Eσ^A-induced permanganate reactivity at −11 (nontemplate strand) and −10 and −12 (template strand) developed to half-maximal levels between 20 and 25 °C while reactivity at −4 did not reach its half-maximal level until 30 °C (Figure 4C). We therefore postulate that a partially melted intermediate is significantly populated under these conditions. This intermediate, designated RP_n, has nucleated melting within the TATA element, but the strand-separation has not extended downstream to −4, the next base which gives a strong signal in this assay.

Transcription of the trnS Operon by B. subtilis RNAP. The above data indicated that open complexes formed more readily at P_{trnS} than at P_{ilv}, at least in the presence of δ. To see if this correlated with increased promoter strength, we first compared the overall rate constant for initiation from P_{trnS} with that for P_{ilv} studied previously (Juang & Helmann, 1994a). The pre-steady-state lag in the rate of RNA synthesis, when transcription is initiated by addition of RNAP to a prewarmed solution of DNA and NTPs, was between 20 and 30 s using the *ilv-leu* leader region as template (Juang & Helmann, 1994a), but no lag was detectable on the 1237 bp fragment containing the *trnS* operon (data not shown). This suggests that the rate of initiation from P_{trnS} is at least 10-fold faster than that at P_{ilv}.

In the course of these experiments, we observed that E$\sigma^A\delta$ was about 5-fold more active than Eσ^A at 40 °C in a multiple-round transcription assay (8 min incubation), despite the inhibitory effect of δ on promoter melting (data not shown). This is consistent with the ability of δ to stimulate transcription of the *ilv-leu* operon, which we attribute to an increased

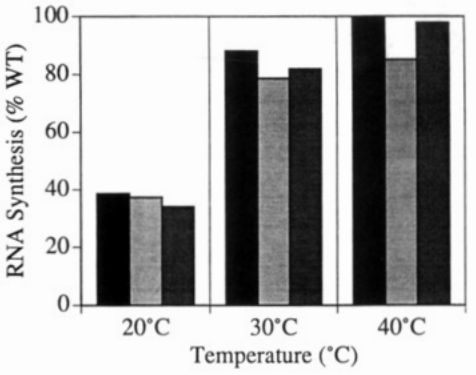

FIGURE 5: Temperature dependence of *in vitro* transcription by mutant E$\delta\sigma^A$ RNAP. RNA product was measured after 8-min incubation using the 1237 bp fragment containing the *trnS* operon (Figure 1) as template. RNAP contained Y189A σ^A (left bar), or W192A σ^A (middle bar), or W193A σ^A (right bar). Activities for each mutant RNAP were normalized to wild type at the same temperature.

efficiency of RNAP recycling (Juang & Helmann, 1994a). In the absence of δ, product RNA appears to bind to RNAP and inhibit recycling. δ can overcome product inhibition, and thereby stimulate transcription, by displacing RNA from RNAP−RNA binary complexes (F. Lopez de Saro and J. D. Helmann, unpublished data).

We next measured the effects of melting-defective σ^A mutants on RNA synthesis from P_{trnS}. We have demonstrated previously that RNAP reconstituted with any of several σ^A region 2.3 mutants is defective in DNA-melting at P_{ilv} (Juang & Helmann, 1994b). As a consequence, the mutant RNAP exhibits reduced activity, relative to a wild-type, when promoter melting is rate-limiting for RNA synthesis. At P_{ilv}, this is true at temperatures below 30 °C under our standard *in vitro* conditions, while recycling is rate-limiting at higher temperatures. Therefore, this in vitro cold sensitivity provides a diagnostic signal of the melting defect.

To determine if σ^A region 2.3 mutants affected transcription initiation from P_{trnS}, we reconstituted RNAP with the Y189A, W192A, or W193A σ^A proteins and assayed activity as a function of temperature. At P_{trnS}, each of these three reconstituted RNAPs was as active as wild type (>65% activity) at both 20 °C and 40 °C (data not shown). In contrast, the reconstituted RNAP mutants containing δ (E$\sigma^A\delta$) were somewhat cold-sensitive (Figure 5), indicating that under these conditions (20 °C, presence of δ) initiation was now rate-limiting for multiple-cycle transcription. When these data are compared against those reported previously for P_{ilv} (Juang & Helmann, 1994a), it is apparent that P_{trnS} behaves as a stronger promoter: the effects of δ and σ^A mutants on the linear P_{trnS} template are qualitatively similar to those observed at P_{ilv} when the DNA is supercoiled.

Effects of σ^A Region 2.3 Mutants on DNA-Melting at P_{trnS}. We next determined the extent and pattern of DNA-melting at P_{trnS} induced by RNAP containing either wild-type σ^A or one of the σ^A region 2.3 mutants (Figure 6 and Table 1). At 40 °C, the wild-type and three mutant holoenzymes were all able to establish open complexes, as judged by the permanganate reactivity of thymines at −4 and −11 (Figure 6), but the σ^A mutants were defective in DNA-melting as judged by a modest decrease in the permanganate signals (between 2- and 5-fold; Table 1). As noted in Figure 3, the −11 signal is relatively weak, but it correlates well with the stronger signals at −10 and −12 on the template strand.

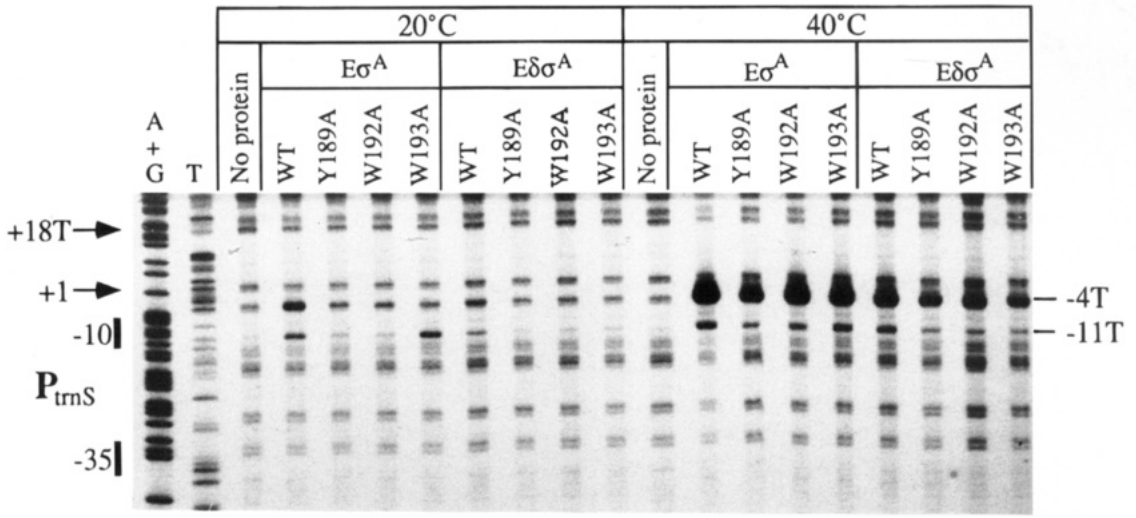

FIGURE 6: Effects of σ^A mutants on promoter melting. RNAP reconstituted with the indicated σ^A mutants (or wild-type σ^A) was incubated with P_{trnS} DNA and the extent of $KMnO_4$ reactivity determined at 20 and 40 °C.

Table 1: Fraction of Maximal $KMnO_4$ Reactivity of RNAP−DNA Complexes Varies with Holoenzyme Composition, Temperature, and Position within the Transcription Bubble[a]

		$E\sigma^A$ holoenzyme				$E\sigma^A$ δ holoenzyme			
temp (°C)	$KMnO_4$ site	WT	Y189A	W192A	W193A	WT	Y189A	W192A	W193A
20	−11T	0.37	0.14	0.07	0.40	0.10	0.04	0.05	0.11
	−4T	0.06	0.02	0.01	0.02	0.02	0	0.01	0.01
40	−11T	1.00	0.22	0.37	0.37	0.37	0.22	0.14	0.16
	−4T	1.00	0.20	0.47	0.37	0.18	0.08	0.08	0.08

[a] The band intensity at −11 and −4 (from Figure 6) was quantitated by PhosphorImaging (Molecular Dynamics) analysis and used to calculate the fraction of maximal reactivity at each position. In absolute terms, the thymine at −4 is 4-fold more reactive than that at −11 at both 20 and 40 °C. The σ^A protein in the holoenzyme was either wild-type or contained a point mutation shown previously to decrease DNA-melting (Juang & Helmann, 1994b).

Therefore, we used this band as a measure of DNA-melting within the TATA region of the promoter (nucleation). At 20 °C, only the wild-type and W193A mutant RNAPs were able to induce significant permanganate reactivity; and those signals were greatly reduced by δ. Quantitation of these data indicates that the W193A $E\sigma^A$ RNAP nucleates melting normally (as judged by the −11 signal at 20 °C) but has not yet extended the transcription bubble to −4 (Table 1). The other two melting-defective σ^A proteins were decreased in both the −11 and −4 signals at both 20 and 40 °C relative to wild-type. Table 1 provides additional data in support of our earlier suggestion that melting in the upstream region (detected at −11) occurs at lower temperatures than melting downstream (detected at −4): for at least three of the four $E\sigma^A$ RNAPs, thymine reactivity at −11 appeared to be at least partially established at 20 °C while reactivity at −4 was negligible.

Sructure of Binary Complexes at P_{trnS}. Each of the binary complexes represented in Figure 6 has also been studied by DNase I footprinting (Figure 7). In every case, the promoter region was quantitatively bound by RNAP; therefore, the low permanganate reactivity at 20 °C in Figure 6 was not due to a lack of RNAP binding but rather reflects the presence of closed complexes. We also noted that the extent of upstream promoter protection was strongly affected by the presence of δ. In all samples lacking δ, the DNase I footprint extended to −110. It is likely that this extended footprint is due to binding of a second RNAP enzyme upstream, and divergently oriented, from that bound at P_{trnS} since the $E\sigma^A$ reactions, but not the $E\sigma^A\delta$ reactions, displayed permanganate sensitivity at thymines −82, −83, and −85 (data not shown). We have never observed transcripts corresponding to this RNAP binding site and do not yet know if it functions as a promoter, tentatively designated P_y, or as a nonproductive RNAP binding site. A similar divergent RNAP binding site, designated P_x, was identified upstream of P_{ilv} (Juang & Helmann, 1994a,b). Like P_x, RNAP bound at P_y was displaced by δ, a protein known to reduce the affinity of RNAP for nonpromoter and weak promoter sites (Achberger *et al.*, 1982; Dobinson & Spiegelman, 1987).

The binary complex footprints observed at P_{trnS} fall into three classes. First, the $E\sigma^A\delta$ RNAP at 20 °C formed closed complexes (Figure 6) with a region of DNase I protection extending from −62 to +1 with weak protection over the −10 region itself. This is similar to the footprints reported for closed complexes at other promoters (Cowing *et al.*, 1989; Kovacic, 1987). In contrast, the $E\sigma^A$ RNAP binary complexes at 20 °C displayed a more complete protection over the −10 region, and the footprint extended both downstream (as far as +6 for wild-type) and upstream (to about −67; although the upstream boundary is somewhat ambiguous due to the presence of P_y). This extension of the DNase I footprint correlates with the nucleation of melting as judged by the −11 permanganate signal. At 40 °C, open complexes were observed (Figure 6), and the DNase I protection now extended from −67 to approximately +20. In addition, −33 regained sensitivity to DNase I, and a hypersensitive site was induced at positions −22 and −23. These complexes correspond to the formation of the open complex, RP_{o1}, as detected by permanganate footprinting.

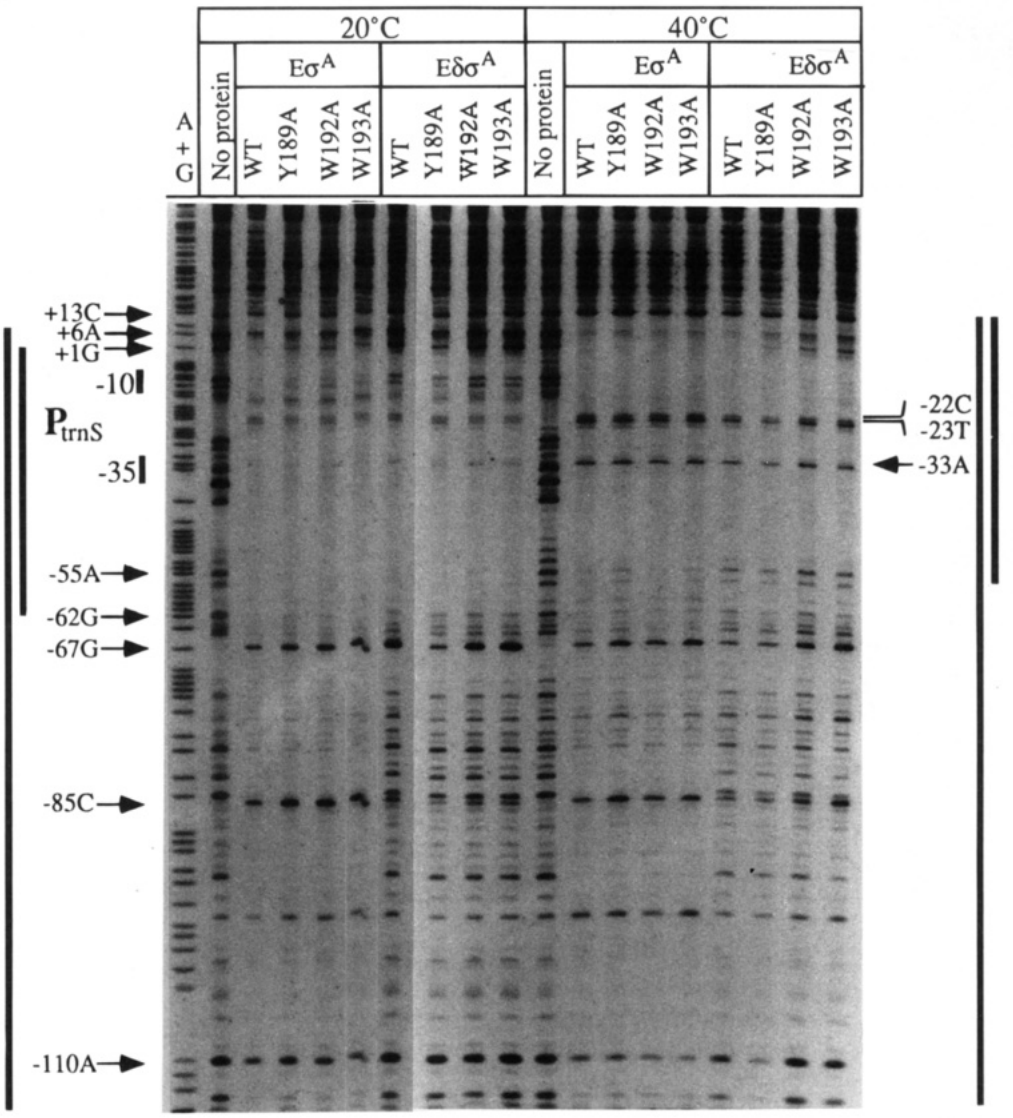

FIGURE 7: DNase I footprinting of P_{trns} binary complexes at 20 and 40 °C. RNAP reconstituted with the indicated σ^A mutants (or wild-type σ^A) was incubated with P_{trnS} DNA as for Figure 6, and the extent of DNase I reactivity was determined. The vertical bars to the left and right of the figure indicate the extent of protection observed in the absence (longer bar) and presence (shorter bar) of δ, at 20 and 40 °C as indicated.

Effects of NTPs on the Pattern of Potassium Permanganate Reactivity of P_{trns}. The open complexes (RP_{o1}) detected at P_{trns} at 40 °C have a DNA-melted region extending from at least −12 to −4 as judged by the permanganate reactivity of thymines. However, we did not observe reactivity of the thymines at −2 and −1 on the nontemplate strand or at −6 and −7 on the template strand. Presumably, the nonreactivity of the template strand −6 and −7 thymines is due to occlusion by bound RNAP; similar nonreactive positions within the boundaries of the transcription bubble have been noted by others (Kainz & Roberts, 1992; Suh *et al.*, 1993). The nonreactivity of the −2 and −1 thymines may also be due to a steric block, or, alternatively, this region may still be double-stranded and thereby define the downstream limit of the transcription bubble.

We reasoned that the binding of the initiating NTP substrates to the RNAP active site might stabilize the transcription bubble in a more open (fully-melted) conformation and thereby allow permanganate reactivity of the thymines flanking the transcription start site (−2, −1, and +2 on the nontemplate strand). Indeed, if GTP, UTP, and CTP were present, RNAP abortively synthesized products up to the 5-mer (data not shown), and thymines at −2, −1, +2, and +4 on the nontemplate strand were now reactive to permanganate (Figure 8). Further, the binding and polymerization of these initiating substrates greatly increased the fraction of DNA-melting observed at 20 °C for wild-type and all three mutant holoenzymes. These results are most simply interpreted as a shift in the equilibrium distribution of complexes from predominantly closed, in the absence of NTPs, to a mixture of closed, open, and transcribing, in the presence of NTPs. This is consistent with the proposal, based on competition experiments, that the various intermediates in transcription initiation are in rapid equilibrium at many *B. subtilis* promoters (Whipple & Sonenshein, 1992).

DISCUSSION

We have investigated complexes formed between *B. subtilis* RNAP and the strong P_{trnS} promoter as a function of solution conditions and the protein composition of the enzyme. These studies confirm the conclusions drawn previously from our analysis of P_{ilv}: the presence of either the δ protein or the selected σ^A region 2.3 mutants decreases the ability of RNAP to melt the promoter. By assuming that

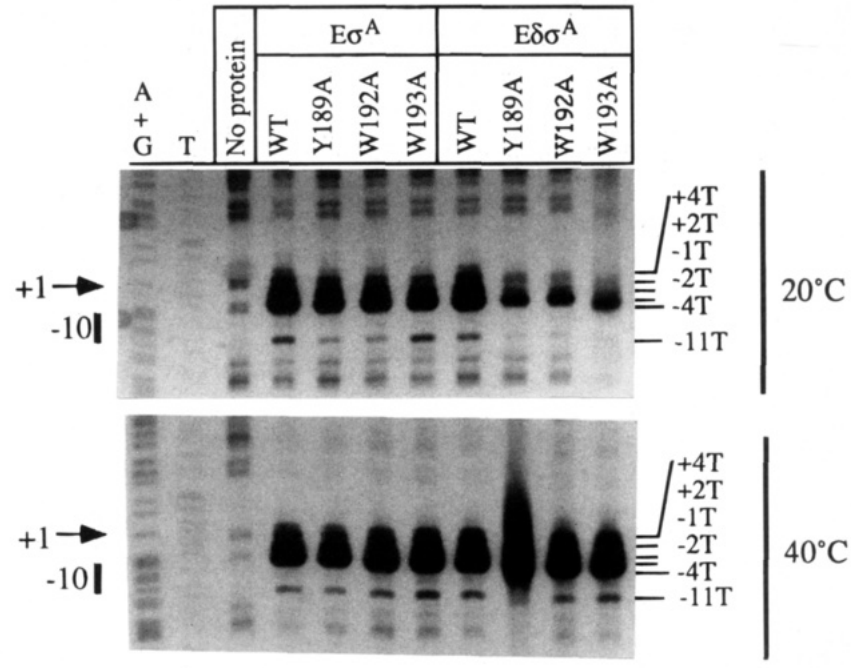

FIGURE 8: Analysis of the effect of phosphodiester bond formation on DNA-melting at 20 and 40 °C. Reactions were performed as in Figure 3 except that 200 μM each of GTP, UTP, and CTP was present. The positions of $KMnO_4$-sensitive thymines are indicated to the right of the figure. The leftmost two lanes are Maxam−Gilbert reactions for A+G and T.

the complexes formed under our *in vitro* conditions are representative of normal intermediates in initiation, we can postulate that transcription from P_{trns} proceeds through a closed complex, an intermediate (nucleated) complex designated RP_n, and one or more open complexes.

Pathway of Open Complex Formation. The pathway leading to transcription initiation has been most thoroughly studied with the *E. coli* σ^{70} holoenzyme which appears to form at least one intermediate, designated RP_i, between the initial recognition complex (RP_c) and the strand-separated open complex (RP_o) (Leirmo & Record, 1990). Evidence for RP_i was obtained at *lac*UV5 when it was found that the rate of RNAP isomerization to inactive complexes upon temperature downshift was much greater than the rate of formation of poly[d(AT)]-sensitive closed complexes (Buc & McClure, 1985). Attempts to characterize RP_i have been hampered by the short lifetime of this species and by the difficulty of synchronizing the RP_c to RP_o transition. As an alternative, several studies have characterized RNAP−promoter complexes as a function of temperature on the assumption that the various stable complexes are likely to mimic the transient intermediates which occur during initiation (Buckle & Buc, 1989; Kirkegaard *et al.*, 1983; Mecsas *et al.*, 1991; Schickor *et al.*, 1990; Spassky *et al.*, 1985). Footprinting studies on *lac*UV5 revealed that RP_i is a closed complex with an extended DNase I footprint (Spassky *et al.*, 1985). Similarly, *E. coli* σ^{32} RNAP bound at the GroEL promoter forms two sequential closed complexes prior to formation of the open complex (Mecsas *et al.*, 1991). These studies have led to the general conclusion that RP_i involves an extension of downstream contacts between RNAP and promoter DNA with little if any strand-separation. The subsequent progression from RP_i to RP_o involves a cooperative melting of the transcription bubble as judged by the steep temperature dependence of RP_o formation (Buc & McClure, 1985; Kirkegaard *et al.*, 1983) and the concurrent increase in the reactivity of various bases within the transcription bubble as the temperature is raised (Buckle & Buc, 1989; Kirkegaard *et al.*, 1983; Spassky *et al.*, 1985).

The mechanisms leading to DNA-melting are unclear. It has been argued that melting probably nucleates within the TATA element (Travers, 1987) since this region is intrinsically unstable. For example, this region is highly reactive to copper orthophenanthroline-mediated cleavage (Spassky *et al.*, 1988), and modifications within the −10 region which artificially create a localized distortion increase open complex formation (Chan *et al.*, 1989; Werel *et al.*, 1991). Despite this circumstantial evidence, direct evidence for a role of the TATA element in the nucleation of DNA-melting has been difficult to obtain. This probably indicates that nucleation is rate-limiting for DNA-melting under most conditions and that once nucleation occurs, the region of DNA-melting rapidly propagates to establish the fully melted transcription bubble (Leirmo & Record, 1990). Some hints that melting may nucleate within the −10 element were obtained with the *gal*P1 promoter: the template strand −11T was found to melt at slightly lower temperatures than +3T (Grimes *et al.*, 1991). This effect is particularly noticeable when a supercoiled template is used (Burns & Minchin, 1994). It has also been shown that σ^{54} RNAP, which requires an activator protein for RP_o formation, forms closed complexes with a localized distortion centered around −12 (Morris *et al.*, 1994). Finally, we note that $KMnO_4$ footprinting of yeast RNA polymerase III complexes indicates a noncooperative melting transition with an upstream region melting at low temperature followed by downstream extension of the transcription bubble at higher temperature (Kassavetis *et al.*, 1992).

Pathway of Open Complex Formation at P_{trnS}. The work presented here indicates that DNA-melting at P_{trnS} can be either concerted (as observed in Tris-HCl buffer) or stepwise (as observed in Na•Hepes buffer). In the latter condition, DNA-melting nucleates within the conserved TATA element. Permanganate reactivity at −11 (nontemplate strand) and

−12 and −10 (template strand) is established at lower temperatures than at −4, which leads us to postulate the existence of a nucleated intermediate, RP_n. RP_n is analogous to RP_i, as postulated for *E. coli* σ^{70} holoenzyme, but is a partially melted intermediate rather than a closed complex. The formation of RP_n is decreased by point mutations in σ^A identified previously as impairing the melting process (Juang & Helmann, 1994b). Both Y189 and W192, but not W193, appear to participate in nucleation since mutants altered in these residues are decreased in −11 reactivity at 20 °C. We argue elsewhere that several of the region 2.3 aromatic amino acids form a melting motif and may stack with exposed bases to stabilize the displaced nontemplate strand (Helmann, 1994; Helmann & Chamberlin, 1988). The functional difference we note between W192 and W193 is also consistent with studies of the corresponding *E. coli* σ^{70} mutants; the residue corresponding to W193 (W434) appears to be in a hydrophobic environment and may play a structural role while the residue corresponding to W192 (W433) is not important for maintaining σ structure, but is important for transcriptional activity (Gopal *et al.*, 1994).

The RP_n to RP_o transition at P_{trnS} involves a downstream extension of DNA contacts and propagation of the single-stranded bubble to at least −4, but apparently not past −2. This step, like nucleation, can be inhibited by δ. Further extension of the transcription bubble, leading to exposure of the −2 and −1 thymines, is only apparent in the presence of NTPs, suggesting that the energy released by NTP binding and perhaps polymerization is needed to stably melt the transcription start site. Similarly, detection of DNA-melting at the start site of *rrnB* P1 requires the two initiating substrates (Newlands *et al.*, 1991). At P_{trnS}, as at other *B. subtilis* promoters (Dobinson & Spiegelman, 1987; Juang & Helmann, 1994a; Rojo *et al.*, 1993; Whipple & Sonenshein, 1992), our data suggest that these various intermediates are in equilibrium and that formation of the transcription bubble occurs in several steps (eq 1):

$$R + P \rightleftharpoons RP_c \underset{\delta}{\overset{\sigma}{\rightleftharpoons}} RP_n \rightleftharpoons RP_o \overset{NTPs}{\rightleftharpoons} RP_{init} \quad (1)$$

It is interesting to note that the effects of σ^A region 2.3 mutants and δ on DNA-melting appear to be independent. For example, at 40 °C, RNAP containing either δ or the W192A mutant σ^A protein is reduced in DNA-melting at −11 to a similar extent (0.37 of control) while the presence of both reduces melting to 0.14 (0.37 × 0.37) of the control (Table 1).

Comparison of P_{trnS} and P_{ilv}. Several similarities are apparent between complexes formed by RNAP at P_{trns} (this work) and P_{ilv} (Juang & Helmann, 1994b). In both cases, δ exhibits an antimelting activity. At P_{ilv}, RNAP containing δ forms predominantly closed complexes even at 40 °C while at P_{trnS} substantial DNA-melting is detected, but the apparent transition temperature is increased by at least 15 °C. The defects imparted by the σ^A region 2.3 mutants on melting of P_{trns}, while not as dramatic as those shown previously for P_{ilv}, are still readily detectable. All three σ^A mutants tested (Y189A, W192A, and W193A) impart a cold-sensitive transcription phenotype when initiation is rate-limiting for multiple cycle transcription. At P_{ilv}, these conditions are met at 20 °C, while at P_{trns} these conditions are met at 20 °C only if δ is present. At both P_{ilv} and P_{trns}, RNAP binds to an upstream, divergently oriented site (P_x and P_y, respectively). Since δ inhibits RNAP binding at this upstream site and inhibits DNA-melting at both P_{ilv} and P_{trns}, it is possible that the upstream RNAP facilitates open complex formation. There is precedence for the idea that upstream RNAP binding sites might play a positive role in transcription from studies of the *E. coli* tyrosine tRNA gene (*tyrT*) (Travers *et al.*, 1982, 1983). Further studies addressing the role of these upstream binding sites in transcription initiation will be presented elsewhere.

REFERENCES

Achberger, E. C., Hilton, M. D., & Whiteley, H. R. (1982) *Nucleic Acids Res. 10*, 2893−2910.

Buc, H., & McClure, W. R. (1985) *Biochemistry 24*, 2712.

Buckle, M., & Buc, H. (1989) *Biochemistry 28*, 4388.

Burns, H., & Minchin, S. (1994) *Nucleic Acids Res. 22*, 3840−3845.

Carpousis, A. J., & Gralla, J. D. (1980) *Biochemistry 19*, 3245−3253.

Chan, P. T., Sullivan, J. K., & Lebowitz, J. (1989) *J. Biol. Chem. 264*, 21277.

Cowing, D. W., Mecsas, J., Record, M. T., Jr., & Gross, C. A. (1989) *J. Mol. Biol. 210*, 521−530.

Dobinson, K. F., & Spiegelman, G. B. (1987) *Biochemistry 26*, 8206−8213.

Ellinger, T., Behnke, D., Bujard, H., & Gralla, J. D. (1994a) *J. Mol. Biol. 239*, 455−465.

Ellinger, T., Behnke, D., Knaus, R., Bujard, H., & Gralla, J. D. (1994b) *J. Mol. Biol. 239*, 466−475.

Garrity, D. B., & Zahler, S. A. (1993) *J. Bacteriol. 175*, 6512−6517.

Garrity, D. B., & Zahler, S. A. (1994) *Genetics 137*, 627−636.

Gopal, V., Ma, H.-W., Kumaran, M. K., & Chatterji, D. (1994) *J. Mol. Biol. 242*, 9−22.

Gourse, R. L. (1988) *Nucleic Acids Res. 16*, 9789−9808.

Grimes, E., Busby, S., & Minchin, S. (1991) *Nucleic Acids Res. 19*, 6113−6118.

Hansen, U. M., & McClure, W. R. (1980) *J. Biol. Chem. 255*, 9564−9570.

Helmann, J. D. (1994) in *Transcription: Mechanisms and Regulation* (Conaway, R. C., & Conaway, J. W., Eds.) pp 1−17, Raven Press, New York.

Helmann, J. D., & Chamberlin, M. J. (1988) *Annu. Rev. Biochem. 57*, 839−872.

Juang, Y.-L., & Helmann, J. D. (1994a) *J. Mol. Biol. 239*, 1−14.

Juang, Y.-L., & Helmann, J. D. (1994b) *J. Mol. Biol. 235*, 1470−1488.

Kainz, M., & Roberts, J. (1992) *Science 255*, 838−841.

Kassavetis, G. A., Blanco, J. A., Johnson, T. E., & Geiduschek, E. P. (1992) *J. Mol. Biol. 226*, 47−58.

Kirkegaard, K., Buc, H., Spassky, A., & Wang, J. C. (1983) *Proc. Natl. Acad. Sci. U.S.A. 80*, 2544−2548.

Knaus, R., & Bujard, H. (1988) *EMBO J. 7*, 2919−2923.

Knaus, R., & Bujard, H. (1990) in *Nucleic Acids and Molecular Biology* (Eckstein, F., & Lilley, D. M. J., Eds.) pp 110−122, Springer-Verlag, Heidelberg.

Kovacic, R. T. (1987) *J. Biol. Chem. 262*, 13654−13661.

Krummel, B., & Chamberlin, M. J. (1989) *Biochemistry 28*, 7829−7842.

Leirmo, S., & Record, M. T., Jr. (1990) in *Nucleic Acids and Molecular Biology* (Eckstein, F., & Lilley, D. M. J., Eds.) Vol. 4, pp 123−151, Springer-Verlag, Heidelberg.

Mecsas, J., Cowing, D. W., & Gross, C. A. (1991) *J. Mol. Biol. 220*, 585−597.

Morris, L., Cannon, W., Claverie-Martin, F., Austin, S., & Buck, M. (1994) *J. Biol. Chem. 269*, 11563.

Munson, L., & Reznikoff, W. S. (1981) *Biochemistry 20*, 2181−2085.

Newlands, J. T., Ross, W., Gosink, K. K., & Gourse, R. L. (1991) *J. Mol. Biol. 220*, 569−583.

Ohlsen, K. L., & Gralla, J. D. (1992a) *J. Biol. Chem. 267*, 19813−19818.
Ohlsen, K. L., & Gralla, J. D. (1992b) *J. Bacteriol. 174*, 6071−6075.
Roe, J. H., Burgess, R. R., & Record, M. T., Jr. (1985) *J. Mol. Biol. 184*, 441−453.
Rojo, F., Nuez, B., Mencia, M., & Salas, M. (1993) *Nucleic Acids Res. 21*, 935−940.
Ross, W., Gosink, K. K., Salomon, J., Igarishi, K., Zou, C., Ishihama, A., Severinov, K., & Gourse, R. L. (1993) *Science 262*, 1407−1413.
Schickor, P., Metzger, W., Werel, W., Lederer, H., & Heumann, H. (1990) *EMBO J. 9*, 2215−2220.
Spassky, A., Kirkegaard, K., & Buc, H. (1985) *Biochemistry 24*, 2723.
Spassky, A., Rimsky, S., Buc, H., & Busby, S. (1988) *EMBO J. 7*, 1871−1879.
Stackhouse, T. M., Telesnitsky, A. P., & Meares, C. F. (1989) *Biochemistry 28*, 7781−7788.
Suh, W.-C., Ross, W., & Record, M. T., Jr. (1993) *Science 259*, 358−361.
Travers, A. A. (1987) *CRC Crit. Rev. Biochem. 22*, 181−219.
Travers, A. A., Lamond, A. I., Mace, H. A., & Berman, M. L. (1983) *Cell 35*, 265−273.
Travers, A. A., Lamond, A. I., & Mace, H. A. (1982) *Nucleic Acids Res. 10*, 5043−5057.
Werel, W., Schickor, P., & Heumann, H. (1991) *EMBO J. 10*, 2589−2594.
Whipple, F. W., & Sonenshein, A. L. (1992) *J. Mol. Biol. 223*, 399−414.

BI950405+